Journal of Quantitative Spectroscopy & Radiative Transfer ▮ (▮▮▮▮) ▮▮▮–▮▮▮

Contents lists available at SciVerse ScienceDirect

Journal of Quantitative Spectroscopy & Radiative Transfer

journal homepage: www.elsevier.com/locate/jqsrt

Optimised frequency grids for infrared radiative transfer simulations in cloudy conditions

G. Holl*, S.A. Buehler, J. Mendrok, A. Kottayil

Division of Space Technology, Department of Computer Science, Electrical and Space Engineering, Luleå University of Technology, Rymdcampus 1, 98128 Kiruna, Sweden

ARTICLE INFO

Article history:
Received 22 March 2012
Received in revised form
31 May 2012
Accepted 31 May 2012

Keywords:
HIRS
AVHRR
Infrared
Radiometer
Radiative transfer
Clouds
Cloudy radiative transfer
Frequency grid

ABSTRACT

This paper shows that radiometer channel radiances for cloudy atmospheric conditions can be simulated with an optimised frequency grid derived under clear-sky conditions. A new clear-sky optimised grid is derived for AVHRR channel 5 (12 μm, 833 cm^{-1}). For HIRS channel 11 (7.33 μm, 1364 cm^{-1}) and AVHRR channel 5, radiative transfer simulations using an optimised frequency grid are compared with simulations using a reference grid, where the optimised grid has roughly 100–1000 times less frequencies than the full grid. The root mean square error between the optimised and the reference simulation is found to be less than 0.3 K for both comparisons, with the magnitude of the bias less than 0.03 K. The simulations have been carried out with the radiative transfer model Atmospheric Radiative Transfer Simulator (ARTS), version 2, using a backward Monte Carlo module for the treatment of clouds. With this module, the optimised simulations are more than 10 times faster than the reference simulations. Although the number of photons is the same, the smaller number of frequencies reduces the overhead for preparing the optical properties for each frequency. With deterministic scattering solvers, the relative decrease in runtime would be even more. The results allow for new radiative transfer applications, such as the development of new retrievals, because it becomes much quicker to carry out a large number of simulations. The conclusions are applicable to any downlooking infrared radiometer.

1. Introduction

Radiative transfer modelling in cloudy atmospheres is an important tool for the development of satellite-based retrievals of cloud properties. Improved retrievals of properties such as Ice Water Path (IWP) are needed, because (ice) clouds are a major source of uncertainty in climate models (e.g. [30, Section 8.6.3.2]). For infrared radiation, a simple simulation of an instrument radiance is computationally expensive, because it requires thousands of monochromatic calculations. However, such a simulation is potentially more accurate than a simulation using band models, because band models include spectral averaging assumptions and parameterise optical properties (e.g. [25,31]). This reduces the flexibility of the model. Therefore, there is a need for a way to reduce calculation times, without compromising on accuracy or flexibility. This is particularly true for cloudy simulations, because a single monochromatic simulation is computationally much more expensive if cloud scattering is taken into consideration.

One way to reduce calculation times is to use an optimised frequency grid. By an optimised frequency grid, we mean a frequency grid that has significantly less (typically 100 to 1000 times less) frequencies than the full reference grid. The derivation of such an optimised

* Corresponding author. Tel.: +46 980 79182; fax: +46 980 79190.
E-mail address: gerrit.holl@ltu.se (G. Holl).

0022-4073/$ - see front matter © 2012 Elsevier Ltd. All rights reserved.
http://dx.doi.org/10.1016/j.jqsrt.2012.05.022

grid for infrared radiances is non-trivial, because it depends on atmospheric composition and viewing geometry, and because the optimisation is highly non-linear (i.e. there are many local minima that are not close to the global minimum). One method to derive an optimised grid is the correlated k method [18]. Another method is based on simulated annealing [6]. The simulated annealing approach is better suited to find a frequency grid that works well for a large variety of atmospheres. The grids used in this study are derived using simulated annealing, but the conclusions also hold for grids derived using other methods.

The primary aim of this study is to show that those clear-sky derived optimised frequency grids can be used for the simulation of cloudy radiances and that calculation times are significantly reduced. Although the spectral dependence of cloud optical properties is much smaller than the spectral dependence of gas absorption properties (as illustrated at the end of this paper), it is not self-evident that a clear-sky derived grid can be used for cloudy simulations. If the signal measured by a satellite-borne sensor is fully dominated by a cloud, the spectrum is flat and the exact choice of an optimised grid is not crucial. This is the situation for a high, thick cloud in a window channel. On the other hand, if the signal is a mixture between a cloudy and a clear-sky one, the situation may be more complicated. For example, if the cloud top is located as the same height as the peak of a broad weighting function for a particular channel, the atmospheric region from which the clear-sky signal originates is affected by the cloud. This means that the absorption due to different gases may be affected in different ways and that their relative contribution to the measured signal may change, which in turn has consequences for the most favourable weighting in an optimised frequency grid. Therefore, it is worth investigating whether the clear-sky derived grid is always a suitable choice for a simulation in the presence of clouds.

The secondary aims of the study are: (1) present a Advanced Very High Resolution Radiometer (AVHRR) setup for the radiative transfer model Atmospheric Radiative Transfer Simulator (ARTS), and (2) present the first cloudy infrared radiometer simulations using ARTS (infrared limb spectra were calculated with ARTS by Hoepfner and Emde [19]).

We focus on High-resolution Infrared Radiation Sounder (HIRS) and AVHRR, because those are sensors on operational satellites. Therefore, they allow for analysis of relatively **long time** series and they have a dense spatial and temporal coverage. However, the conclusions are valid of any downlooking infrared radiometer.

For cloudy simulations, we use a backward Monte Carlo model [12]. Nevertheless, the conclusions are applicable to any radiative transfer solver. The present study serves as a demonstration of the method.

More discussion on the validity of the conclusions follows later in the paper.

The structure of the paper is as follows. In Section 2, we describe the sensors, the radiative transfer model and the data used in the study. In Section 3, we describe the experiments we have carried out to test if the optimised grid derived using clear-sky simulations is valid for cloudy simulations as well. The results of those experiments are presented in Section 4 and discussed in Section 5. We finish in Section 6 by concluding remarks and a discussion of future work.

2. Methodology

2.1. Sensors

AVHRR is a downlooking imager in the visible/infrared that has been flown on polar-orbiting satellites from National Oceanic and Atmospheric Administration (NOAA) and MetOp since the late 1970s. It has a wide variety of atmospheric and non-atmospheric applications [11,24]. On the latest generation, AVHRR/3, channels 4 (10.8 μm, 926 cm^{-1}) and 5 (12 μm, 833 cm^{-1}) are window channels in the thermal infrared.

HIRS is a downlooking infrared sounder for temperature and humidity [33], carried on many operational satellites. It carries 20 channels ranging from the visible up to wavelengths of 15 μm (667 cm^{-1}).

In this study, we use a window channel and a sounding channel, in order to test our method under different conditions. For the window channel, we use AVHRR channel 5. For the sounding channel, we use HIRS channel 11, centred at 7.33 μm (1364 cm^{-1}) and with a Jacobian peaking in the mid-troposphere (varying in height depending on atmospheric humidity).

2.2. Radiative transfer simulations

2.2.1. ARTS

ARTS is a flexible and powerful model for the simulation of radiances at thermal infrared, sub-millimeter and microwave frequencies [3,16]. ARTS can perform radiative transfer simulations in one, two, or three dimensions and can consider full polarisation [13]. It performs monochromatic pencil-beam simulations and can convolve spectral irradiances with a sensor response function (SRF) to calculate instrument radiances. It can also consider the instrument antenna pattern. The implementation of ARTS infrared continua is described by Buehler et al. [4].

ARTS has been used for a wide variety of applications. For example, it has been used for the analysis of operational microwave satellite measurements [2,22,23,28,29], for sensor capability studies of future sub-millimeter radiometers [5,8,21,32], and for the modelling of infrared radiative transfer [4,19,26].

ARTS implements various optimisations to reduce calculation time, without significantly compromising accuracy. The sensor response is efficiently modelled by a matrix multiplication [15]. Atmospheric absorption can be treated by an absorption lookup table [7]. For radiance simulations of channels containing many spectral lines, such as channels on the infrared sensors HIRS and AVHRR, a large number of monochromatic simulations needs to be calculated in order to fully characterise the channel radiance. Buehler et al. [6] have developed a method to derive a small set of frequencies with associated weights that accurately represent the channel radiance. This allows the user to reduce the number of

Please cite this article as: Holl G, et al. Optimised frequency grids for infrared radiative transfer simulations in cloudy conditions. J Quant Spectrosc Radiat Transfer (2012), http://dx.doi.org/10.1016/j.jqsrt.2012.05.022

monochromatic radiance calculations by a factor of roughly 100–1000. This in turn dramatically decreases the calculation time without introducing any significant errors in the calculated channel radiance. Thus, it becomes possible to quickly perform a large number of simulations, as required to get good statistics, to develop new retrievals, or to do retrievals. Buehler et al. [6] have derived optimised frequency grids for HIRS and under clear-sky conditions only. We show that the optimised grid produces results as accurate as the reference grid, even for cloudy simulations.

2.2.2. Cloudy radiative transfer

ARTS is able to perform radiance simulations in the presence of scattering particles, such as ice particles. Two alternative modules for calculating cloudy radiances are included.

One is the Discrete Ordinate ITerative (DOIT) module [14,34]. DOIT is a polarised Discrete Ordinate Method (DOM). DOIT has been developed for microwave and submillimeter radiances, where ice particle scattering phase functions are quite smooth. For infrared radiation, ice particle scattering phase functions have a strong forward peak (e.g. [9,35]). To properly characterise this with a DOM, a very fine angular grid is required, which makes the simulations very slow and therefore impractical. Although methods exist to alleviate this problem, none are currently implemented in ARTS-DOIT.

The other scattering module is a backward Monte Carlo (MC) method [12]. MC is often slower than DOM, but in the presence of a strong forward peak, MC was found to be faster for the problem at hand. For each monochromatic pencil-beam simulation, photons are generated, traced, and a radiance is calculated. This continues until either (1) a desired accuracy is reached, (2) a maximum number of photons is reached, or (3) a time limit is reached.

Although we use a MC-based method for cloudy simulations, the conclusions are valid for any solver. This is further discussed in Section 5.

2.3. Atmospheric data

For this study, we use two datasets containing atmospheric samples.

Firstly, we use atmospheric states from Garand et al. [17], which contain pressure, temperature, and concentrations for water vapour (H_2O), ozone (O_3), carbon dioxide (CO_2), nitrous oxide (N_2O), carbon monoxide (CO), and methane (CH_4). This dataset is clear-sky only.

Secondly, we use a dataset developed by Chevallier et al. [10]. This dataset is suitable for testing purposes, because it

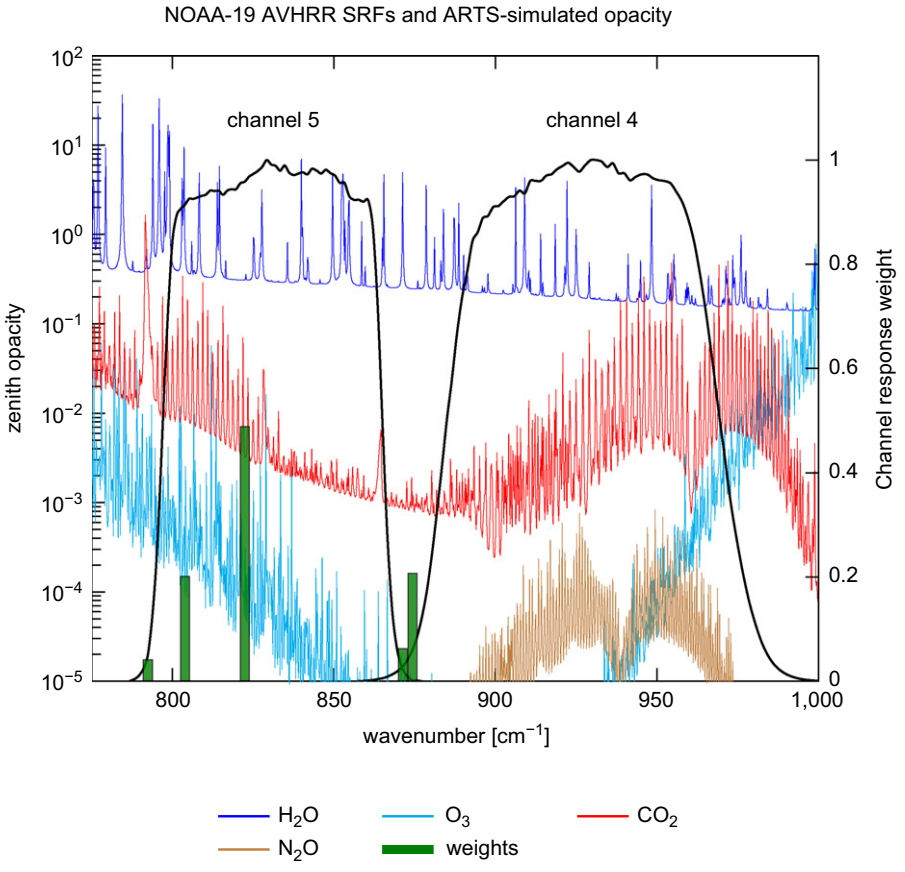

Fig. 1. AVHRR SRF for channels 4 and 5. The figure also shows zenith opacities for the gases that are most strongly affecting channel radiances, as well as the derived frequencies and associated weights for the optimised frequency grid for channel 5. See also Table 1 for a full listing of frequencies and weights. (For interpretation of the references to color in this figure caption, the reader is referred to the web version of this article.)

Please cite this article as: Holl G, et al. Optimised frequency grids for infrared radiative transfer simulations in cloudy conditions. J Quant Spectrosc Radiat Transfer (2012), http://dx.doi.org/10.1016/j.jqsrt.2012.05.022

contains many different atmospheric states, including common and extreme cases. It consists of diverse atmospheric profiles, selected from reanalysis of the European Centre for Medium-range Weather Forecasting (ECMWF). We will refer to this as the Chevallier dataset. The dataset consists of several collections of 5000 profiles, each selected to maximise variability in a particular parameter: temperature, humidity, ozone, cloud condensate and precipitation. The datasets are sorted such that common cases, close to the mean atmospheric state, occur near the start of the dataset, whereas extreme cases occur near the end of the dataset. The total number of profiles is 25,000.

The Chevallier dataset includes profiles of cloud ice water and other hydrometeors. This is unusual, as most well-documented datasets of atmospheric profiles are clear-sky only. Regarding trace gases, it contains volume mixing ratios for water vapour and ozone. To accurately model infrared radiances, profiles for additional atmospheric gases are required, because they affect channel radiances (see Fig. 1). From the US standard atmosphere given by Anderson et al. [1], we have obtained profiles for carbon dioxide (CO_2), nitrous oxide (N_2O), carbon monoxide (CO), methane (CH_4), nitrogen (N_2), and oxygen (O_2), because those gases are present in the dataset from Garand et al. [17], but not in the Chevallier dataset. For those gases, we have used the same profile in every simulation. This does not affect the result, because those gases are either well-mixed or spectroscopically inactive in the region considered in this study.

3. Optimised infrared cloudy radiative transfer

3.1. Clear-sky derivation for AVHRR

We derive an optimised grid for AVHRR) channel 5 (12.0 μm, 833 cm^{-1}) on NOAA-19 (there are small differences in the SRF between different copies of AVHRR). This channel is arbitrary chosen and serves only as an example; the method is applicable to any thermal infrared channel. We use the 42 profiles from Garand et al. [17] described earlier, and set volume mixing ratios for oxygen (O_2) and nitrogen (N_2) to 0.2095 and 0.7808, respectively. The derivation depends on atmospheric composition, so it is important that the atmospheric data represent considerable variability. The derivation is done for clear-sky conditions. No antenna pattern is applied, but all simulations are pencil-beam. All simulations are for a nadir-looking geometry. Surface emissivity is set to one. The reference setup consists of a spectrum ranging from 23.5681 THz (12.72 μm; 786 cm^{-1}) to 26.2981 THz

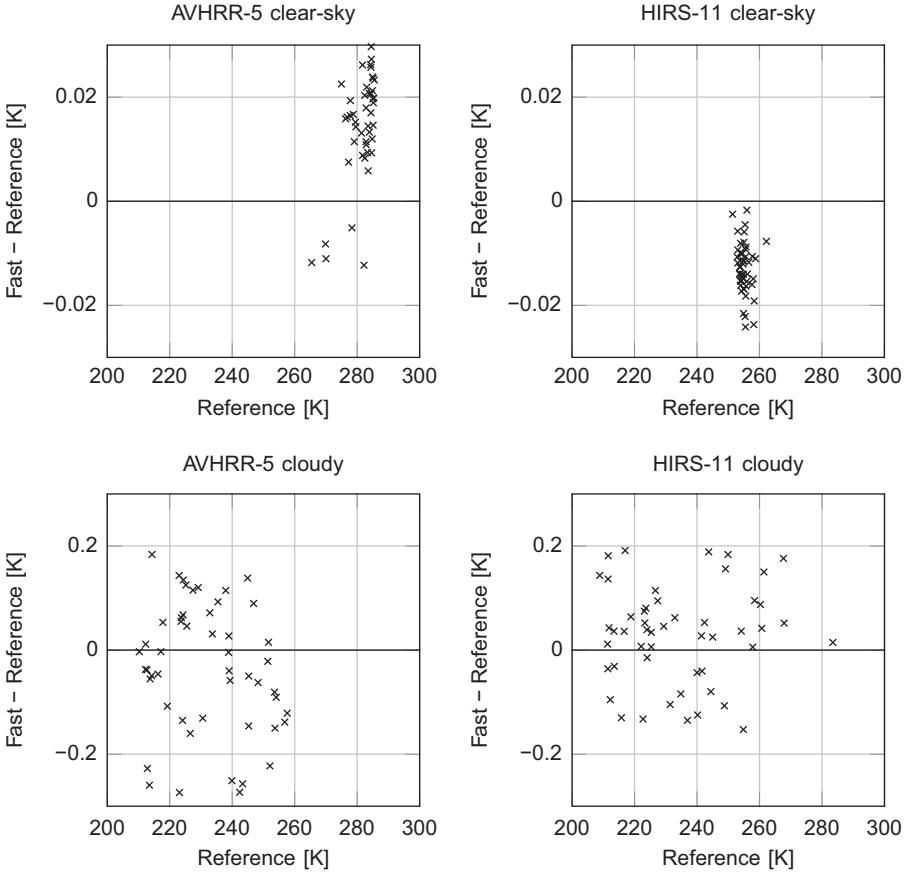

Fig. 2. Comparison between simulations using the optimised and the reference grid. The top row shows the comparison for clear-sky simulations. The bottom row shows the comparison for cloudy simulations (note the difference in *y*-scale). For the cloudy simulations, for each profile, we took the mean of the 10 optimised runs and the mean of the 10 reference runs, and plotted the difference as a function of the mean reference radiance.

Please cite this article as: Holl G, et al. Optimised frequency grids for infrared radiative transfer simulations in cloudy conditions. J Quant Spectrosc Radiat Transfer (2012), http://dx.doi.org/10.1016/j.jqsrt.2012.05.022

(11.40 μm; 877 cm^{-1}), with a constant grid spacing of 5×10^8 Hz (0.016 cm^{-1}). In total, the reference grid is described by 5461 frequencies. Further decreasing the grid spacing does not affect the simulated channel radiance, so this is a sufficient number of frequencies. We derive an optimised frequency grid such that the relative error in the intensity (in $W\,m^{-2}\,Hz^{-1}\,sr^{-1}$) is at most 1×10^{-3}. This corresponds to a brightness temperature of approximately 0.07 K. To determine how many frequencies the optimised grid needs to contain, the procedure is repeated while increasing the number of frequencies, starting with five, until the condition stated above is met.

3.2. Cloudy test for AVHRR and HIRS

To investigate if the optimised frequency grid can be used for the simulation of cloudy radiances, we calculate radiances for a set of 50 cloudy atmospheres using both the reference grid and the optimised grid. The number 50 was chosen as a compromise between calculation speed and sufficient statistics, because the simulation for the reference grid takes a long time (see also Table 2). The atmospheres are from the Chevallier dataset [10] described earlier. We select each 100th profile (profile number 0, 100, ...,4900) from the dataset that maximises variability in cloud condensate. Because of the way the dataset is sorted, choosing each 100th profile provides an appropriate slice-through of the total variability represented by the 5000 profiles (as shown by the full range of brightness temperatures in Fig. 2).

For this study, we include only cloud ice, i.e. no precipitation and no liquid water clouds. We assume the particle size distribution from McFarquhar and Heymsfield [27]. We arbitrarily choose a particle shape of solid hexagonal columns [35]. This does not affect the result, because the physical considerations are similar for other shapes (see Section 5).

As with the simulations used to derive the optimised frequency grid, all simulations are pencil-beam and nadir-looking and surface emissivity is set to one.

We perform simulations for AVHRR channel 5 and HIRS channel 11 using the reference grid and the optimised grid. The number of frequencies for each grid is given in Table 1. Cloudy simulations are carried out using a Monte Carlo solver. The optimised setup consists of 100 photons per frequency for HIRS and 1000 photons per frequency for AVHRR, corresponding to a total number of 1900 and 5000 photons for the channel radiance, respectively. For both sensors, the reference setup simulation uses 10 photons per frequency corresponding to 46,110 photons for HIRS and 54,610 photons for AVHRR.

The error in the simulations consists of two components: (1) the grid error, or the error between the optimised and the full grid, and (2) the Monte Carlo error due to the stochastic nature of the simulation. It is important to distinguish between the two kinds of error, because type (1) is independent of radiative transfer solver, whereas type (2) is specific for the Monte Carlo method.

To investigate the MC error and runtimes for different numbers of photons, we repeat each simulation 10 times with identical input. By MC error, we mean the variability of the calculated brightness temperatures between subsequent runs with identical input. This variability arises from the random nature of MC simulations. This investigation will show if the numbers of photons used in the reference and the optimised runs are sufficient. A simulation with the optimised grid requires a larger number of photons per frequency than a simulation with the reference grid, in order for the total number of photons and therefore the MC error to be similar. However, to limit computation time, the number of photons should not be more than necessary. The number of photons for any simulation – with the reference grid or with the optimised grid – is a tradeoff between computation time and accuracy.

Table 1
List of frequencies and weights for the optimised grid. The grid for Advanced Very High Resolution Radiometer (AVHRR) channel 5 is a new result, whereas the grid for High-Resolution Infrared Radiation Sounder (HIRS) channel 11 was obtained by Buehler et al. [6].

Channel	AVHRR-5		HIRS-11	
reference	5461 Frequencies		4611 Frequencies	
optimised	Freq. (cm^{-1})	Weight	Freq. (cm^{-1})	Weight
	792.40	0.408	1329.686	0.047
	803.91	0.201	1329.919	0.015
	822.42	0.489	1332.420	0.006
	871.31	0.062	1334.921	0.049
	874.29	0.207	1336.739	0.067
			1342.925	0.031
			1347.477	0.045
			1348.411	0.051
			1350.862	0.068
			1351.946	0.031
			1364.169	0.062
			1364.202	0.009
			1369.371	0.103
			1370.605	0.188
			1376.808	0.007
			1385.496	0.082
			1386.496	0.032
			1397.735	0.003
			1400.102	0.105

4. Results

We find that AVHRR channel 5 (henceforth: AVHRR-5) can be represented using a set of only five frequencies. In Fig. 1, the green bars show the frequencies and associated weights that accurately represent the channel radiance (relative error in radiance less than 1×10^{-3}). The full list of frequencies and associated weights is also given in Table 1.

4.1. Accuracy of the optimised grid

For the cloudy simulations for both AVHRR-5 and HIRS channel 11 (henceforth: HIRS-11), we perform a number of tests to investigate the differences between the radiances calculated with the optimised grid and the radiances calculated with the reference grid. Some of those tests are presented here.

Please cite this article as: Holl G, et al. Optimised frequency grids for infrared radiative transfer simulations in cloudy conditions. J Quant Spectrosc Radiat Transfer (2012), http://dx.doi.org/10.1016/j.jqsrt.2012.05.022

Fig. 2 shows the differences between the optimised and the reference grid as a function of mean reference radiances. For the clear-sky simulations, AVHRR-5 has a small positive bias whereas HIRS-11 has a small negative bias. For the cloudy simulations, the situation is the opposite. For cloudy AVHRR-5, the bias between the optimised and the reference setup is -0.032 K. The bias is similarly small for the runs with HIRS-11. In both cases, the cloudy bias is not a function of radiance.

Fig. 3 shows a histogram of the data presented in Fig. 2. The figure presents a histogram of the error of the radiance obtained with the optimised grid compared to the radiance obtained with the reference grid, and a histogram of the error due to the random nature associated solely with the Monte Carlo simulation method. Since both the reference-grid simulations and the optimised-grid simulations use the Monte Carlo method, both histograms include the Monte Carlo error. The two histograms look very similar and no outliers with a large error are present. This means that most of the variability in the error between radiances simulated with the optimised or the reference grid is due to the Monte Carlo error (maximum error around 1 K), and not due to errors introduced by the optimised frequency grid (root mean square error less than 0.03 K).

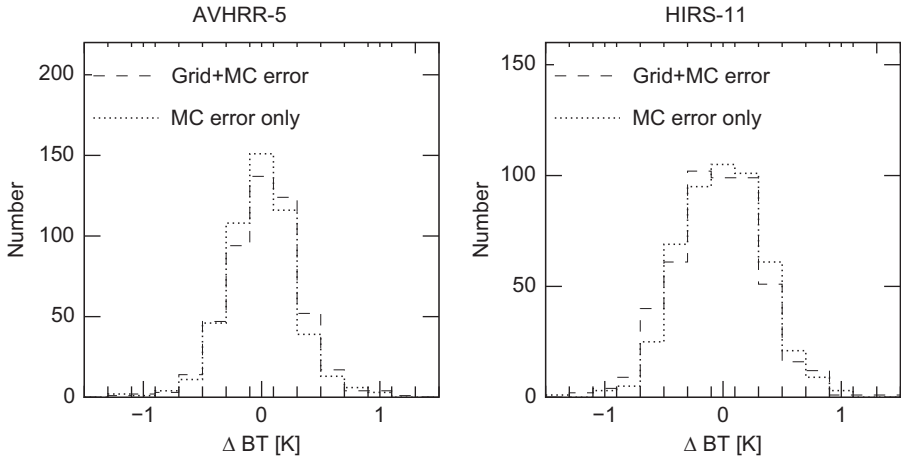

Fig. 3. Error statistics for the error due to the optimised frequency grid and the random nature of Monte Carlo simulations, for AVHRR-5 and High-resolution Infrared Radiation Sounder (HIRS)-11. The dashed line (- - -) shows the radiance obtained with the optimised grid minus the mean radiance obtained with the reference grid. This describes the sum of Monte Carlo error and grid error. The dotted line (.....) shows the radiance obtained with the optimised grid minus the mean radiance obtained with the optimised grid. This describes purely the Monte Carlo error.

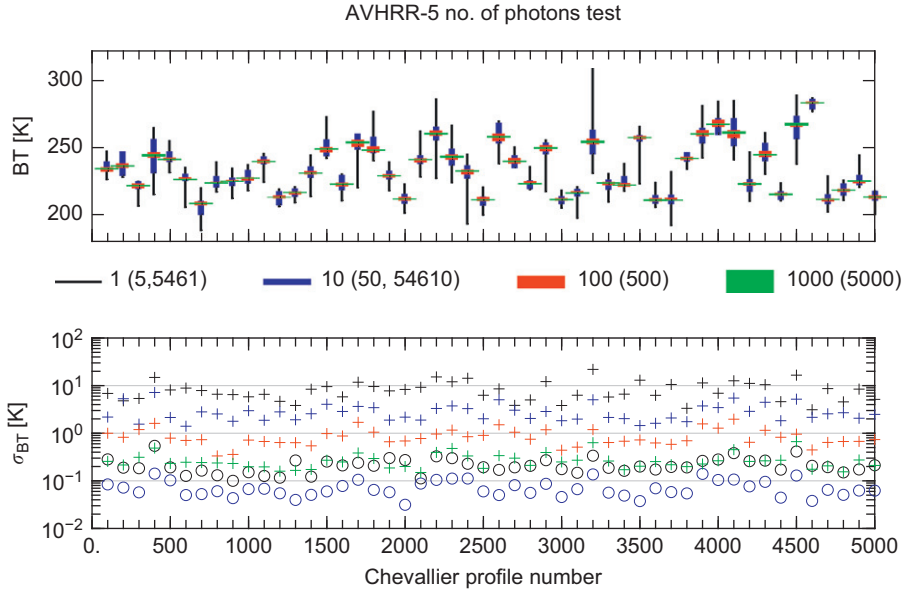

Fig. 4. Variability of brightness temperatures for 10×50 cloudy simulations as described in the text for AVHRR-5. The top panel shows the range of brightness temperatures for the optimised run on the lower panel, the pluses show the standard deviations for 10 optimised runs, while the circles show the standard deviation for 10 reference runs. The legend shows the number of photons per frequency. In brackets are the total number of photons for the optimised grid and the reference grid, respectively.

Please cite this article as: Holl G, et al. Optimised frequency grids for infrared radiative transfer simulations in cloudy conditions. J Quant Spectrosc Radiat Transfer (2012), http://dx.doi.org/10.1016/j.jqsrt.2012.05.022

We also investigate the difference as a function of the column mass density of ice through the cloud (not shown), but we do not find any significant pattern.

We conclude that the optimised frequency grid, derived for clear-sky conditions, can be used even for cloudy atmospheres.

4.2. Monte Carlo-specific runtime considerations

Monte Carlo simulations have a specific relation between number of frequencies, runtime, and accuracy. This is different for deterministic scattering solvers, where runtime per channel is proportional to the number of frequencies and the error does not depend on the number of simulations. As we use a MC solver in the present study (for technical reasons), we investigate how runtime and accuracy depend on the number of photons per frequency and per channel. In Section 5 we discuss the wider implications of the results obtained with the Monte Carlo solver.

Even with the optimised grid, Monte Carlo simulations are expensive. We investigate how many photons per frequency are needed to reduce the MC error to an acceptable level yet obtain a simulation runtime that allows for doing hundreds to thousands of simulations, as needed e.g. for developing or doing retrievals. We do so for both the optimised and the reference grid, because it is not a priori obvious that the optimised grid is faster. Since the optimised grid operates on a much smaller number of frequencies, the number of photons per frequency needs to be much higher in order to keep the MC error low, as the MC error is determined by the total number of photons for the channel radiance.

Figs. 4 and 5 show the MC error for AVHRR and HIRS for a varying number of photons per frequency, respectively. Unsurprisingly, the brightness temperatures converge and the variability goes down as the number of photons increases. The highest standard deviation for the AVHRR runs for the 50 selected atmospheres is 1.972 K for the runs with 500 photons and 0.666 K for the run with 5000 photons. A standard deviation of 2 K is still rather high, but a standard deviation of 0.7 K is acceptable for many applications. The standard deviations for the AVHRR reference setup with 5461 photons in total (1 per frequency) are similar to those for the optimised setup with 5000 photons. The HIRS runs show a similar pattern.

In practice, the MC error is not the only consideration for choosing the setup. For most applications, a large number of scenarios need to be simulated. Therefore, the runtime per simulation is of major practical importance.

Table 2 shows the time the simulations took to run on an Intel(R) Xeon(R) X5482 Dual QuadCore (8 CPUs) with 3.20 GHz CPU and 16 GiB RAM. It shows that runtime increases with the number of photons, but not quite linearly in the studied range. For a small number of photons per frequency, runtime increases less than linearly with the number of photons, particularly when the number

Table 2
Time to simulate 50 cloudy atmospheres for AVHRR channel 5 using ARTS-MC. "s" is seconds, "m" is minutes, and "h" is hours. User time refers to the real time passed during the simulation. CPU time refers to the processor time. On a multi-core machine running parallelised code, CPU time may be considerably larger than user time.

Run	Photons		Time			
	Per freq.	Total	User		cpu	
			min	Median	min	Median
Optimised (5 freq.)	1	5	39 s	43 s	2 m	2 m
	10	50	4 m	4 m	12 m	13 m
	100	500	19 m	36 m	2 h	2 h
	1000	5000	3 h	3 h	15 h	15 h
Reference (5461 freq.)	1	5461	74 h	74 h	97 h	97 h
	10	54,610	77 h	77 h	238 h	239 h

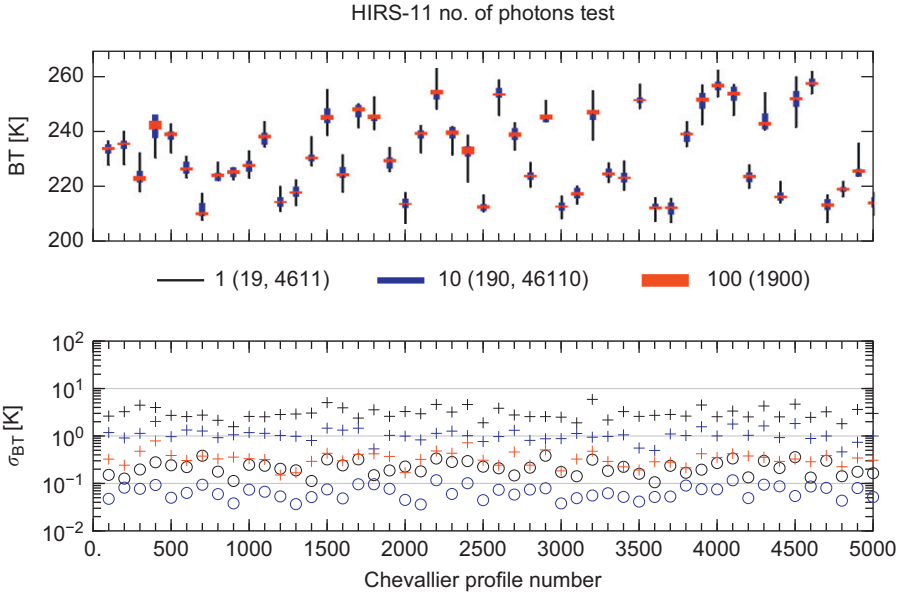

Fig. 5. As Fig. 4, but for HIRS-11.

Please cite this article as: Holl G, et al. Optimised frequency grids for infrared radiative transfer simulations in cloudy conditions. J Quant Spectrosc Radiat Transfer (2012), http://dx.doi.org/10.1016/j.jqsrt.2012.05.022

of frequencies to simulate is large. For approximately the same total number of photons (5000), the optimised setup is still much faster than the reference setup. Therefore the optimised setup is a good choice for doing simulations.

5. Discussion

There are several reasons why the clear-sky derived optimised frequency grid can be used for cloudy simulations. Buehler et al. [6] require all weights to be to be (1) positive, (2) inside the channel, and (3) to add up to be exactly equal to one. These requirements make the result more consistent with our physical understanding of the problem, and if the spectrum is flat, a weighted mean gives the same result as a simple mean. Figs. 6 and 7 show calculated spectra for a window channel (AVHRR-5) and a sounding channel (HIRS-11), respectively. For both figures, panel (a) shows the spectrum for a thick cloud with a high cloud top height, whereas panel (b) shows the spectrum for a relatively low and thin ice cloud. Clear-sky spectral radiances vary strongly as a function of wavelength, because of the high number of relatively narrow spectral lines in the infrared. This effect is stronger for the sounding channel (Fig. 7) than for the window channel (Fig. 6). For a high and thick cloud, radiances emerge mostly from the cloud top. Since cloud optical properties are not strongly spectrally dependent, the spectrum for such a profile is quite flat. This can be seen in Figs. 6a and 7a. The spectrum for a profile with a low and thin cloud is much less flat. For the window channel (Fig. 6b), the spectrum is still relatively flat, although strong lines are apparent. The spectrum for the sounding channel with a low

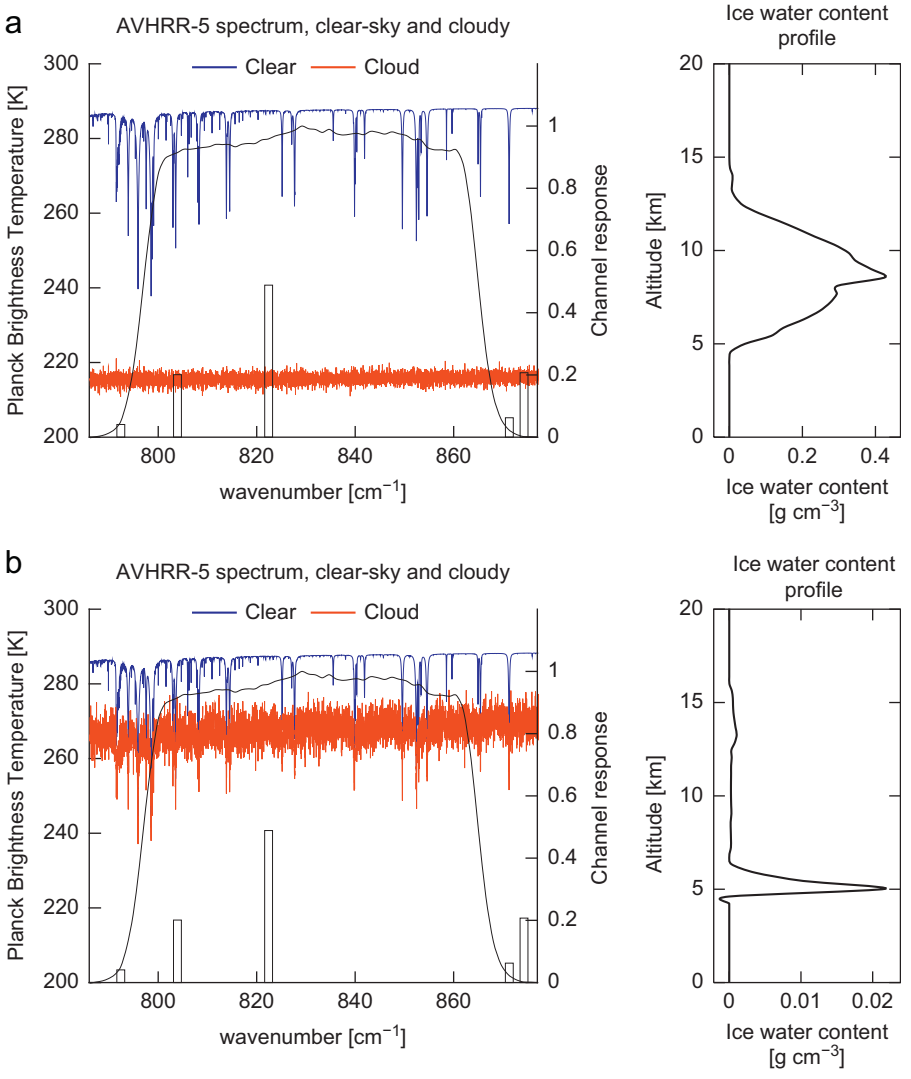

Fig. 6. Infrared nadir-looking spectra for wavelengths in AVHRR channel five for atmospheric profiles 4300 (panel a) and 4400 (panel b) from the Chevallier dataset [10]. The IWC profiles are shown for reference. Channel response and weights are repeated from Fig. 1. The noise in the cloudy spectrum is due to the limited number of photons per frequency. Although 100 photons per frequency is more than enough to simulate the channel radiance using the full frequency grid (it would mean around 500,000 photons), there is still significant noise at each individual frequency. Due to constraints on computation power and time, a reference calculation with significantly more photons is not feasible: (a) Chevallier profile 4300 and (b) Chevallier profile 4400.

Please cite this article as: Holl G, et al. Optimised frequency grids for infrared radiative transfer simulations in cloudy conditions. J Quant Spectrosc Radiat Transfer (2012), http://dx.doi.org/10.1016/j.jqsrt.2012.05.022

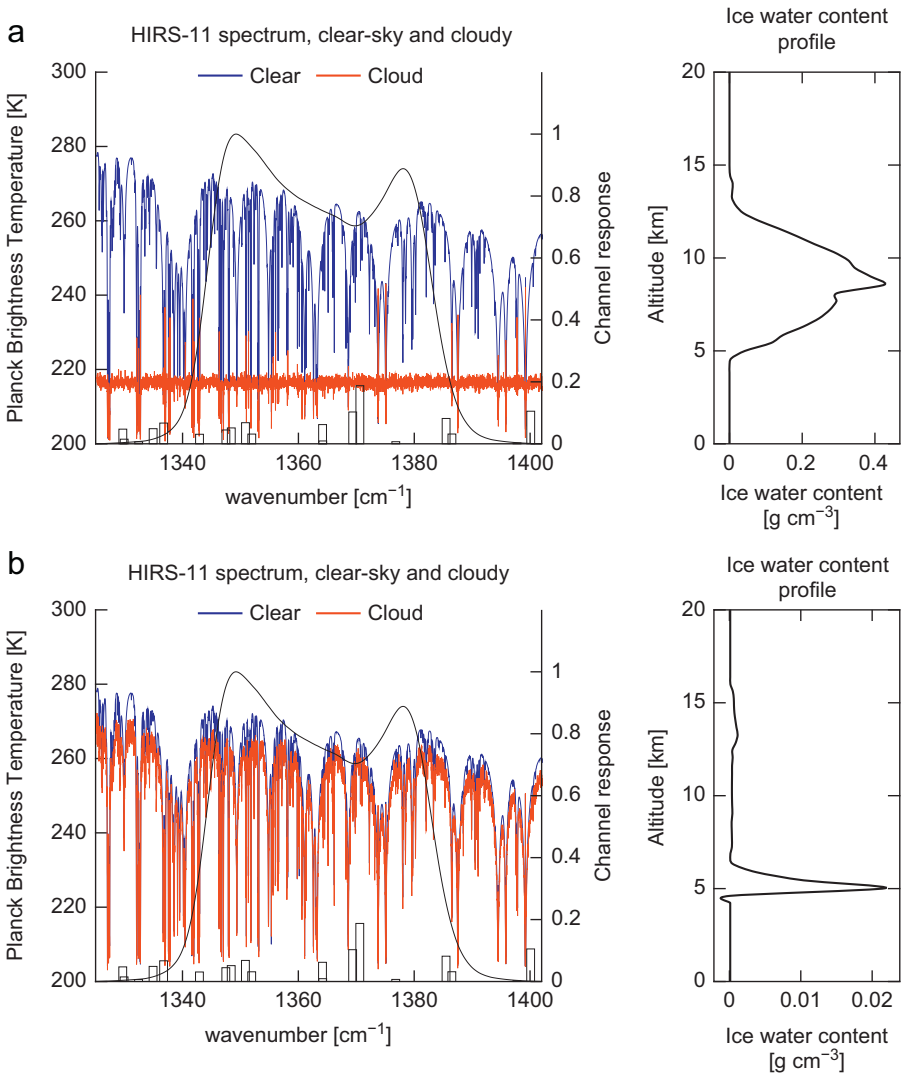

Fig. 7. As Fig. 6, but for HIRS-11: (a) Chevallier profile 4300 and (b) Chevallier profile 4400.

and thin cloud (Fig. 7b) is almost the same as for the clear-sky, because the signal originates mainly from the atmosphere above the cloud.

As discussed in the introduction, a more difficult situation may arise if the cloud top coincides with the peak of a broad weighting function. In this case, the atmospheric region from which the clear-sky signal originates changes, and therefore the relative contribution for different gases might, too. However, we find that the optimised grid works for all explored cases.

When considering clouds only, many combinations of frequencies and associated weights work, as long as the weights add up to one and the slight variation of optical properties with frequency is represented. Since gaseous absorption and emission still occur in a cloudy sky, also above the cloud, the clear-sky-derived optimised frequency grid is a good choice for cloudy simulations.

The time gain by using an optimised frequency grid with a Monte Carlo model is less than the time gain with a deterministic scattering solver. In fact, that there is a time difference at all between 5000 photons distributed over a large number of frequencies or the same number distributed over a small number of frequencies can be explained by the overhead associated with preparing the MC simulation for each frequency. Some tasks, such as extracting optical properties, need to be performed once for each frequency.

The time gain for deterministic scattering solvers is expected to be much larger. For such models, the runtime per channel is (close to) directly proportional to the total number of frequencies per channel. Therefore, an optimised frequency grid will give a reduction in runtime by a factor 100 to 1000.

6. Conclusions and outlook

In this study, we have shown that an optimised frequency grid derived for clear-sky conditions with the

Please cite this article as: Holl G, et al. Optimised frequency grids for infrared radiative transfer simulations in cloudy conditions. J Quant Spectrosc Radiat Transfer (2012), http://dx.doi.org/10.1016/j.jqsrt.2012.05.022

method described by Buehler et al. [6] can be applied for cloudy simulations. For a newly derived optimised frequency grid for AVHRR channel 5 and a frequency grid derived by Buehler [6] for HIRS channel 11, we have investigated the differences between simulations using the optimised grid and the full grid, respectively. The optimised grid has 100–1000 times less frequencies than the full grid. We found the bias to be less than 0.03 K with no dependence on cloud properties.

For simulations with a deterministic scattering solver, it is evident that reducing the number of frequencies decreases the runtime. However, in the present study, we used the ARTS Monte Carlo model for the simulations. Therefore, we also studied how the choice of the number of photons affects the Monte Carlo errors and runtimes. For a similar number of photons per channel, the optimised grid has the same accuracy as the reference grid, but is approximately 10 times faster.

The results can be applied to any downlooking infrared radiometer and are highly useful for further studies.

Like the optimised HIRS frequency grids developed by Buehler et al. [6], the new optimised frequency grid for AVHRR channel 5 is available along with the ARTS software distribution.

We plan to apply the results, for example, to a systematic study of the IWP signal in AVHRR thermal radiances. Such a study would compare statistics with those from a collocated dataset based on Holl et al. [20] (further developed by John et al. [23]) and those for microwave radiances, in particular Microwave Humidity Sounder (MHS) channels around the 183 GHz water vapour absorption line. This study might be carried out in the future.

Acknowledgments

The PhD student position of the main author is funded by the Swedish *Vetenskapsrådet*. We thank Ping Yang for providing the authors with updated single scattering data for the infrared. We thank the ARTS radiative transfer community for its work on ARTS. We would also like to thank the National Graduate School in Space Technology at Luleå University of Technology for offering courses and workshops that helped the PhD student and first author in his research.

References

[1] Anderson GP, Clough SA, Kneizys FX, Chetwynd JH, Shettle EP. AFGL atmospheric constituent profiles (0–120 km). Technical report, AFGL, TR-86-0110; 1986.

[2] Buehler SA, John VO. A simple method to relate microwave radiances to upper tropospheric humidity. J Geophys Res 2005;110: D02110, http://dx.doi.org/10.1029/2004JD005111.

[3] Buehler SA, Eriksson P, Kuhn T, von Engeln A, Verdes C. ARTS, the atmospheric radiative transfer simulator. J Quant Spectrosc Radiat Transfer 2005;91:65–93, http://dx.doi.org/10.1016/j.jqsrt.2004.05.051.

[4] Buehler SA, von Engeln A, Brocard E, John VO, Kuhn T, Eriksson P. Recent developments in the line-by-line modeling of outgoing longwave radiation. J Quant Spectrosc Radiat Transfer 2006;98: 446–57, http://dx.doi.org/10.1016/j.jqsrt.2005.11.001.

[5] Buehler SA, Jiménez C, Evans KF, Eriksson P, Rydberg B, Heymsfield AJ, Stubenrauch C, Lohmann U, Emde C, John VO, Sreerekha TR, Davis CP. A concept for a satellite mission to measure cloud ice water path and ice particle size. Quart J R Meteorol Soc 2007;133: 109–28, http://dx.doi.org/10.1002/qj.143.

[6] Buehler SA, John VO, Kottayil A, Milz M, Eriksson P. Efficient radiative transfer simulations for a broadband infrared radiometer – combining a weighted mean of representative frequencies approach with frequency selection by simulated annealing. J Quant Spectrosc Radiat Transfer 2010;111:602–15, http://dx.doi.org/10.1016/j.jqsrt.2009.10.018.

[7] Buehler SA, Eriksson P, Lemke O. Absorption lookup tables in the radiative transfer model ARTS. J Quant Spectrosc Radiat Transfer 2011;112:1559–67, http://dx.doi.org/10.1016/j.jqsrt.2011.03.008.

[8] Buehler SA, Defer E, Evans F, Eliasson S, Mendrok J, Eriksson P, Lee C, Jimenéz C, Prigent C, Crewell S, Kasai Y, Bennartz R, Gasiewski AJ. Observing ice clouds in the submillimeter spectral range: the CloudIce mission proposal for ESA's earth explorer 8. Atmos Meas Tech Discus 2012;5:1101–51, http://dx.doi.org/10.5194/amtd-5-1101-2012, URL 〈 http://www.atmos-meas-tech-discuss.net/5/1101/2012/〉.

[9] Buras R, Dowling T, Emde C. New secondary-scattering correction in DISORT with increased efficiency for forward scattering. J Quant Spectrosc Radiat Transfer 2011;112:2028–34, http://dx.doi.org/10.1016/j.jqsrt.2011.03.019.

[10] Chevallier F, Di Michele S, McNally AP. Diverse profile datasets from the ECMWF 91-level short-range forecasts. Technical report, NWP SAF satellite application facility for numerical weather prediction. Document no. NWPSAF-EC-TR-010, Version 1.0; 2006.

[11] Cracknell AP. The advanced very high resolution radiometer. CRC Press; 1997.

[12] Davis C, Emde C, Harwood R. A 3D polarized reversed Monte Carlo radiative transfer model for mm and sub-mm passive remote sensing in cloudy atmospheres. IEEE Trans Geosci Remote Sens 2005;43:1096–101, http://dx.doi.org/10.1109/TGRS.2004.837505.

[13] Davis CP, Evans KF, Buehler SA, Wu DL, Pumphrey HC. 3-D polarised simulations of space-borne passive mm/sub-mm midlatitude cirrus observations: a case study. Atmos Chem Phys 2007;7:4149–58, http://dx.doi.org/10.5194/acp-7-4149-2007.

[14] Emde C, Buehler SA, Davis C, Eriksson P, Sreerekha TR, Teichmann C. A polarized discrete ordinate scattering model for simulations of limb and nadir longwave measurements in 1D/3D spherical atmospheres. J Geophys Res 2004;109:D24207, http://dx.doi.org/10.1029/2004JD005140.

[15] Eriksson P, Ekström M, Melsheimer C, Buehler SA. Efficient forward modelling by matrix representation of sensor responses. Int J Remote Sens 2006;27:1793–808, http://dx.doi.org/10.1080/01431160500447254.

[16] Eriksson P, Buehler SA, Davis CP, Emde C, Lemke O. ARTS, the atmospheric radiative transfer simulator. Version 2. J Quant Spectrosc Radiat Transfer 2011;112:1551–8, http://dx.doi.org/10.1016/j.jqsrt.2011.03.001.

[17] Garand L, et al. Radiance and jacobian intercomparison of radiative transfer models applied to HIRS and AMSU channels. J Geophys Res 2001;106:24,017–31.

[18] Goody R, West R, Chen L, Crisp D. The correlated-k method for radiation calculations in nonhomogeneous atmospheres. J Quant Spectrosc Radiat Transfer 1989;42:539–50.

[19] Hoepfner M, Emde C. Comparison of single and multiple scattering approaches for the simulation of limb-emission observations in the mid-IR. J Quant Spectrosc Radiat Transfer 2005;91:275–85, http://dx.doi.org/10.1016/j.jqsrt.2004.05.066.

[20] Holl G, Buehler SA, Rydberg B, Jiménez C. Collocating satellite-based radar and radiometer measurements—methodology and usage examples. Atmos Meas Tech 2010;3:693–708, http://dx.doi.org/10.5194/amt-3-693-2010.

[21] Jiménez C, Buehler SA, Rydberg B, Eriksson P, Evans KF. Performance simulations for a submillimetre wave cloud ice satellite instrument. Quart J R Meteorol Soc 2007;133:129–49, http://dx.doi.org/10.1002/qj.134.

[22] John VO, Buehler SA. Comparison of microwave satellite humidity data and radiosonde profiles: a survey of european stations. Atmos Chem Phys 2005;5:1843–53, http://dx.doi.org/10.5194/acp-5-1843-2005 sRef-ID:1680-7324/acp/2005-5-1843.

[23] John VO, Holl G, Buehler SA, Candy B, Saunders RW, Parker DE. Understanding inter-satellite biases of microwave humidity sounders using global simultaneous nadir overpasses. J Geophys Res 2012;117:D02305, http://dx.doi.org/10.1029/2011JD016349.

[24] Karlsson, KG. An introduction to remote sensing in meteorology, SMHI, ISBN 91-87996-08-1; 1997.

[25] Key JR, Schweiger AJ. Tools for atmospheric radiative transfer: STREAMER and FLUXNET. Comput Geosci 1998;24:443–51, http://dx.doi.org/10.1016/S0098-3004(97)00130-1.

Please cite this article as: Holl G, et al. Optimised frequency grids for infrared radiative transfer simulations in cloudy conditions. J Quant Spectrosc Radiat Transfer (2012), http://dx.doi.org/10.1016/j.jqsrt.2012.05.022

[26] Kottayil A, Buehler SA, John VO, Miloshevich LM, Milz M, Holl G. On the importance of Vaisala RS92 radiosonde humidity corrections for a better agreement between measured and modeled satellite radiances. J Atmos Ocean Technol 2012;29:248–59, http://dx.doi.org/10.1175/JTECH-D-11-00080.1.

[27] McFarquhar GM, Heymsfield AJ. Parameterization of tropical cirrus ice crystal size distribution and implications for radiative transfer: results from CEPEX. J Atmos Sci 1997;54:2187–200.

[28] Melsheimer C, Heygster G. Improved retrieval of total water vapor over polar regions from AMSU-B microwave radiometer data. IEEE Trans Geosci Remote Sens 2008;46:2307–22, http://dx.doi.org/10.1109/TGRS.2008.918013.

[29] Moradi I, Buehler SA, John VO, Reale A. Evaluating inhomogeneities in global radiosonde upper tropospheric humidity data using microwave satellite data. J Geophys Res, submitted for publication.

[30] Randall DA, Wood RA, Bony S, Colman R, Fichefet T, Fyfe J, et al. Climate models and their evaluation. In: Solomon S, Qin D, Manning M, Chen Z, Marquis M, Averyt KB, Tignor M, Biller HL, editors, Climate change 2007: the physical science basis. Contribution of working group I to the fourth assessment report of the intergovernmental panel on climate change, Cambridge, United Kingdom, New York, NY, USA: Cambridge University Press; 2007.

[31] Richiazzi P, Yang S, Gautier C, Sowle D. SBDART: a research and teaching software tool for plane-parallel radiative transfer in the earths atmosphere. Bull Am Meteorol Soc 1998;79:2101–14, http://dx.doi.org/10.1175/1520-0477(1998)079〈2101:SARATS〉2.0.CO;2.

[32] Rydberg B, Eriksson P, Buehler SA. Prediction of cloud ice signatures in sub-mm emission spectra by means of ground-based radar and in-situ microphysical data. Quart J R Meteorol Soc 2007;133:151–62, http://dx.doi.org/10.1002/qj.151.

[33] Smith WL, Bishop WP, Dvorak VF, Hayden CM, McElroy JH, Mosher FR, Oliver VJ, Purdom JF, Wark DQ. The meteorological satellite: overview of 25 years of operation. Science 1986;231:455–62.

[34] Sreerekha TR, Buehler SA, Emde C. A simple new radiative transfer model for simulating the effect of cirrus clouds in the microwave spectral region. J Quant Spectrosc Radiat Transfer 2002;75:611–24.

[35] Yang P, Wei H, Huang H-L, Baum BA, Hu YX, Kattawar GW, Mishchenko MI, Fu Q. Scattering and absorption property database for nonspherical ice particles in the near- through far-infrared spectral region. Appl Opt 2005;44:5512–23, http://dx.doi.org/10.1364/AO.44.005512.

Please cite this article as: Holl G, et al. Optimised frequency grids for infrared radiative transfer simulations in cloudy conditions. J Quant Spectrosc Radiat Transfer (2012), http://dx.doi.org/10.1016/j.jqsrt.2012.05.022